NACA RM L55B11

[redacted]

Copy 6
RM L55B11

RESEARCH MEMORANDUM

COMPARISON OF THE STATIC STABILITY OF A 68.7° DELTA-WING MODEL WITH DIHEDRAL AND A TWISTED AND CAMBERED WING MODEL OF THE SAME PLAN FORM

By John W. Paulson

Langley Aeronautical Laboratory
Langley Field, Va.

NATIONAL ADVISORY COMMITTEE
FOR AERONAUTICS

WASHINGTON
April 7, 1955

[redacted]

NATIONAL ADVISORY COMMITTEE FOR AERONAUTICS

RESEARCH MEMORANDUM

COMPARISON OF THE STATIC STABILITY OF A 68.7° DELTA-WING MODEL WITH DIHEDRAL AND A TWISTED AND CAMBERED WING MODEL OF THE SAME PLAN FORM

By John W. Paulson

SUMMARY

A force-test investigation has been conducted in the Langley free-flight tunnel to determine whether the static stability characteristics of a twisted and cambered 68.7° delta wing could be approximated by a plane wing of similar plan form with dihedral. Such an investigation was of interest because static tests of a twisted and cambered wing model showed that the model had high directional stability in the high angle-of-attack range. It was found in the present investigation that values of directional stability approximately equal to those of the twisted and cambered wing could be obtained with dihedral angles of 20° or 30°.

INTRODUCTION

Interest has recently been shown in the use of twist and camber in the wing as a means of minimizing the pressure peaks at the design lift coefficient that usually occur on low-aspect-ratio highly swept wings in supersonic flight (ref. 1). In other investigations (for example, ref. 2), it has been shown that twist and camber also provide a means for delaying leading-edge separation of high-speed wing configurations to higher lift-coefficients than for the plane wing. An investigation (ref. 3), conducted in the Langley stability tunnel to determine the low-speed lift-drag and static stability characteristics of a delta and a highly tapered sweptback wing with twist and camber, showed that these wings became directionally stable at high angles of attack. Other recent investigations (for example, ref. 4) have shown that plane wings of similar plan form generally experience a severe loss in directional stability at high angles of attack. Since this large loss in directional stability is very undesirable, the use of twist and camber becomes of interest from a stability standpoint because it appears to offer a means of eliminating this loss in stability.

Since twisted and cambered wings are structurally complex, other means of obtaining their desirable stability characteristics more simply were considered. Preliminary analysis showed that the beneficial effects of the twisted and cambered wing could be attributed to an effective geometric dihedral which resulted in the wing having large side area behind the center of gravity. It was decided, therefore, to use in the present investigation a plane-wing model in which the dihedral could be varied. The model had 68.7° sweepback of the leading edge which corresponded to the plan form of the twisted and cambered wing of references 1 and 3. The dihedral of the wing could be varied along a line parallel to the fuselage center line and tangent to the fuselage at its maximum thickness; the dihedral of the outer portion of the wing could be varied along a sweep line of about 77°. Provisions were made for varying the inboard and outboard dihedrals in combination so that the model gave a more accurate geometrical representation of the twisted and cambered wing. The characteristics of the twisted and cambered model of reference 3 were also determined for comparison purposes.

SYMBOLS

The data are presented in the form of standard NACA coefficients of forces and moments which are referred in all cases to the stability axes with the origin at the quarter-chord point of the mean aerodynamic chord. The coefficients are based on the geometry of the wing at 0° dihedral. The positive directions of the forces, moments, and angular displacements are shown in figure 1. The coefficients and symbols used herein are defined as follows:

C_L lift coefficient, Lift/qS

C_D drag coefficient, Drag/qS

C_Y lateral-force coefficient, Lateral force/qS

C_m pitching-moment coefficient, Pitching moment/$qS\bar{c}$

C_l rolling-moment coefficient, Rolling moment/qSb

C_n yawing-moment coefficient, Yawing moment/qSb

L lift, lb

D drag, lb

X	longitudinal force, lb
Y	lateral force, lb
M	pitching moment, ft-lb
L'	rolling moment, ft-lb
N	yawing moment, ft-lb
q	dynamic pressure, lb/sq ft
V	airspeed, ft/sec
S	wing area, sq ft
b	wing span, ft
A	aspect ratio, $\frac{b^2}{S}$
λ	sweepback, deg
$\bar{c}$	mean aerodynamic chord, ft
t	time, sec
α	angle of attack of reference axis (fig. 1), deg
ψ	angle of yaw, deg
β	angle of sideslip, deg
Γ_o	outboard dihedral, deg
Γ_i	inboard dihedral, deg

$$C_{Y_\beta} = \frac{\partial C_Y}{\partial \beta}$$

$$C_{n_\beta} = \frac{\partial C_n}{\partial \beta}$$

$$C_{l_\beta} = \frac{\partial C_l}{\partial \beta}$$

APPARATUS AND MODEL

The model was tested on a six-component strain-gage balance in the Langley free-flight tunnel which is a low-speed tunnel having a 12-foot octagonal test section. The tunnel was designed primarily for flying dynamically scaled models but force-testing equipment has been installed so that the aerodynamic characteristics of models can be obtained.

A three-view drawing of the 68.7° delta-wing model used in the investigation is presented in figure 2 and the dimensional characteristics are given in table I. The model was built so that the dihedral could be varied along a line parallel to the model center line and tangent to the fuselage at its maximum thickness. The dihedral of the outer portion of the wing could be varied negatively along a sweep line of 77°. The model had a half-delta vertical tail.

TESTS

Force tests were made to determine the static longitudinal stability characteristics of the plane-wing model for angles of attack from 0° to 36° with 0°, 10°, 20°, and 30° inboard dihedral and with 0° outboard dihedral. The longitudinal characteristics were also determined for these same inboard dihedrals with equal and opposite outboard dihedral angles. For the same combinations of inboard and outboard dihedral angles, the static lateral stability characteristics were determined with vertical tail off and on for angles of attack from 0° to 36° at $\pm 5^{\circ}$ sideslip and at an angle of attack of 28° over a sideslip range of $\pm 20^{\circ}$. In a few instances at $\alpha = 28^{\circ}$, outboard dihedral angles up to -60° were tested. In the present investigation, the twisted and cambered wing model of reference 3 was tested for angles of attack from 0° to 36° at sideslip angles of 0° to $\pm 5^{\circ}$.

All force tests were made at a dynamic pressure of 3.2 pounds per square foot which corresponds to an airspeed of about 52 feet per second at standard sea-level conditions and to a Reynolds number of approximately 440,000 based on the wing mean aerodynamic chord of 1.33 feet. All moment data are referred to the center-of-gravity position at 25 percent of the mean aerodynamic chord.

RESULTS AND DISCUSSION

Longitudinal Characteristics

A comparison of the longitudinal characteristics of the plane-wing model with various inboard dihedral angles and those of the twisted and cambered wing model is presented in figure 3. The data show the twisted and cambered wing model had a higher maximum lift coefficient and generally had a higher lift-curve slope over the angle-of-attack range than the plane-wing model with 0° dihedral. As the dihedral was increased on the plane wing, the lift-curve slope decreased and the maximum lift coefficient was reduced by nearly 30 percent.

The longitudinal stability of the plane-wing model with 0° dihedral was slightly less than that of the twisted and cambered wing and the longitudinal stability parameter $C_{m_{\alpha}}$ decreased progressively as the dihedral was increased.

Presented in figure 4 are the longitudinal characteristics of the plane-wing model for several combinations of inboard and outboard dihedral compared with those of the twisted and cambered wing model. These data show that the lift-curve slope and maximum lift coefficient were reduced for all combinations of dihedral angles but the reductions are not as large as those for inboard dihedral only. The longitudinal stability was about the same as that of the model with only inboard dihedral.

Lateral Characteristics

Twisted and cambered wing model.- The data of figure 5 show the variation of the static lateral stability derivatives $C_{Y_{\beta}}$, $C_{n_{\beta}}$, and $C_{l_{\beta}}$ with angle of attack for the twisted and cambered wing model and also for the plane-wing model with various inboard dihedral angles. The twisted and cambered wing model with vertical tail off had approximately neutral directional stability $C_{n_{\beta}}$ at low angles of attack and $C_{n_{\beta}}$ increased rather rapidly to fairly high positive values at an angle of attack of about 28°. At higher angles of attack the directional stability decreased to about half its maximum value. With the vertical tail on, the directional stability increased at angles of attack up to the stall ($\alpha = 33^{\circ}$) but decreased beyond the stall.

The effective dihedral was positive over the angle-of-attack range and reached a maximum value well below the stall. In general, the vertical tail had little influence on the effective dihedral at any angle of attack.

Effect of inboard dihedral on plane-wing model.- The effect of inboard dihedral on the static lateral stability characteristics of the model with tail off over the angle-of-attack range is shown in figure 5. The wing-fuselage combination with 0° dihedral became directionally stable at medium angles of attack and remained slightly stable until the stall when it became very unstable. This increase in directional stability in going from low to medium angles of attack is characteristic of a highly swept wing or wing-fuselage combination in which the fuselage is relatively small, such as in the case of the present model. (See ref. 4.) The amount of directional stability for this configuration at high angles of attack was much less than that of the twisted and cambered wing. Increasing the dihedral to 10° resulted in a large increase in the directional stability, particularly at the higher angles of attack, and the model did not become unstable until after the stall. A further increase in dihedral to 20° to 30° caused further increases in directional stability up to the stall and the model was directionally stable beyond the stall. Since estimates of the center-of-pressure location based on the values of C_{n_β} and C_{Y_β} showed that the center of pressure remained at about 0.2 to 0.25 spans behind the center of gravity at moderate to high angles of attack, the increase in stability with increase in dihedral angles can probably be attributed mainly to the increased side area which also increased the side-force parameter C_{Y_β} as shown in figure 5. With 20° and 30° dihedral, the model approximated the high-angle-of-attack characteristics of the twisted and cambered wing model. The plane-wing model, however, had much larger values of directional stability at low and moderate angles of attack.

The effective dihedral parameter $-C_{l_\beta}$ increased greatly with increasing angle of attack and remained positive over the angle-of-attack range. Increasing the geometric dihedral increased the effective dihedral at low and moderate angles of attack but in the high angle-of-attack range the effect of geometric dihedral was generally small and somewhat erratic. The maximum value of effective dihedral was about the same as that for the twisted and cambered wing, but the values at low and moderate lift coefficients for the wing with dihedral were somewhat larger.

With a vertical tail on, the directional stability increased at angles of attack up to the stall and decreased at angles of attack beyond the stall.

Effect of combinations of inboard and outboard dihedral.- Presented in figure 6 are the variations of C_Y, C_n, and C_l with angle of sideslip for the plane-wing model at an angle of attack of 28° with various inboard and outboard dihedral angles. These data are included to show the nonlinearity of the curves. Presented in figure 7 are the variations of C_{n_β} and C_{l_β} with angle of attack for several dihedral configurations

compared with those for the twisted and cambered wing. The data show that, at high angles of attack, values of directional stability comparable with those of the twisted and cambered wing were achieved with several different dihedral configurations. Using outboard dihedral resulted in a fairly large reduction in directional stability because of the loss in effective side area. The data show that the variation of the effective dihedral parameter with angle of attack was generally similar to that of the twisted and cambered wing for all configurations, but there were large differences in the values at a given angle of attack.

CONCLUSIONS

An investigation to determine the static stability characteristics of a 68.7° delta-wing model with various combinations of inboard and outboard dihedral showed that the model had large values of directional stability with tail off or on at high angles of attack and 20° or 30° of dihedral. These conditions resulted in values of directional stability at high angles of attack comparable with those for the twisted and cambered wing model.

Langley Aeronautical Laboratory,
National Advisory Committee for Aeronautics,
Langley Field, Va., January 27, 1955.

REFERENCES

1. Brown, Clinton E., and Hargrave, L. K.: Investigation of Minimum Drag and Maximum Lift-Drag Ratios of Several Wing-Body Combinations Including a Cambered Triangular Wing at Low Reynolds Numbers and at Supersonic Speeds. NACA RM L51E11, 1951.

2. Hunton, Lynn W.: Effects of Twist and Camber on the Low-Speed Characteristics of a Large-Scale 45° Swept-Back Wing. NACA RM A50A10, 1950.

3. Fisher, Lewis R.: Low-Speed Static Longitudinal and Lateral Stability Characteristics of Two Low-Aspect-Ratio Wings Cambered and Twisted To Provide a Uniform Load at a Supersonic Flight Condition. NACA RM L51C20, 1951.

4. Goodman, Alex, and Thomas, David F., Jr.: Effects of Wing Position and Fuselage Size on the Low-Speed Static and Rolling Stability Characteristics of a Delta-Wing Model. NACA TN 3063, 1954.

TABLE I.- GEOMETRIC CHARACTERISTICS OF THE MODEL

Wing:	
Sweepback, deg	68.7
Airfoil section parallel to plane of symmetry	NACA 0002
Aspect ratio	1.56
Area (total to center line), sq in.	225
Span, in.	18.72
Mean aerodynamic chord, in.	16
Fuselage:	
Length, in.	32
Maximum thickness (19 inches from nose), in.	3.12
Vertical tail (fuselage):	
Sweepback, deg	60
Airfoil section	1/8-inch flat plate
Aspect ratio (exposed area)	1.15
Area (exposed), sq in.	21.7
Span (above fuselage), in.	5.0
Root chord, in.	8.7
Mean aerodynamic chord, in.	5.75

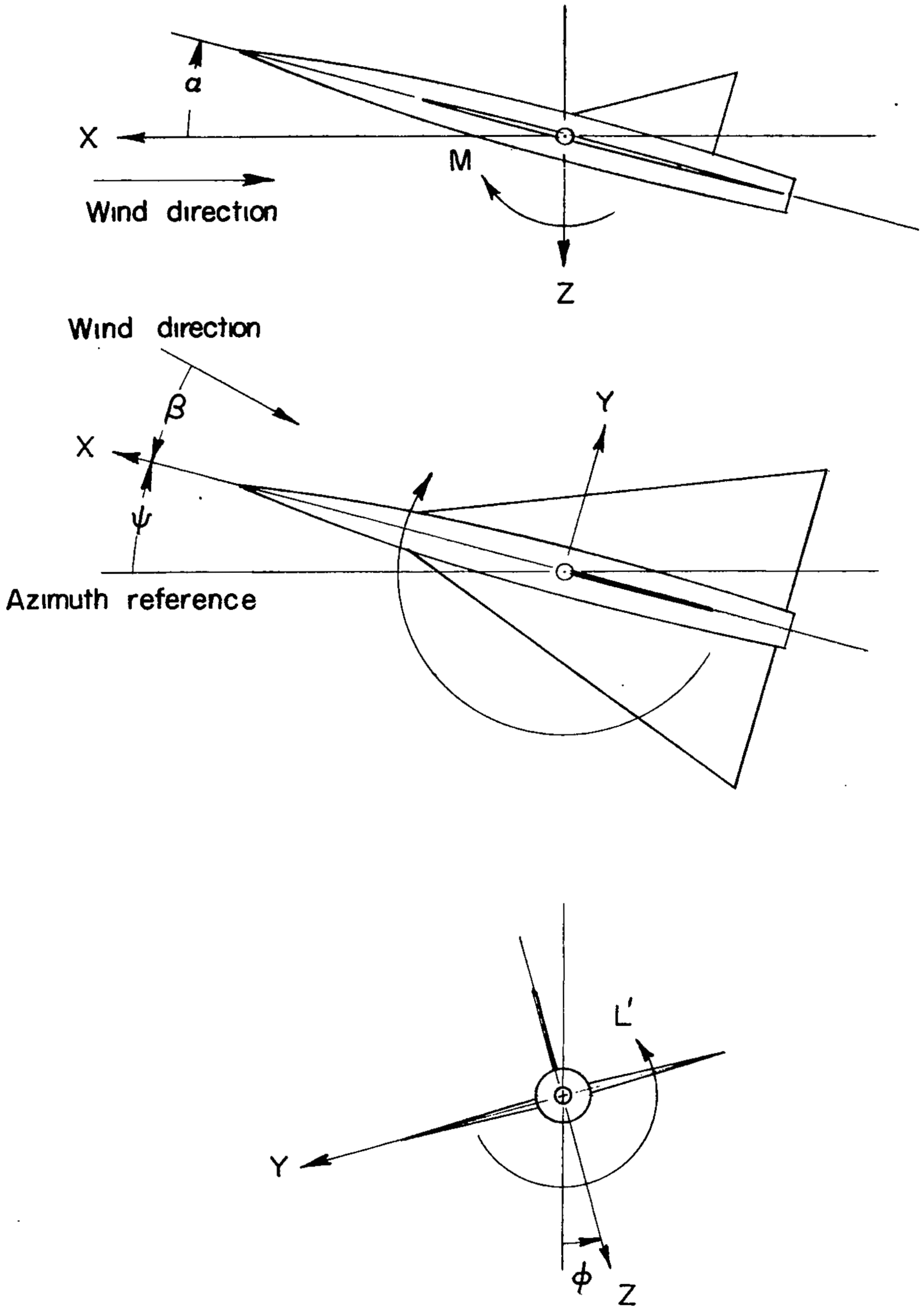

Figure 1.- The stability system of axes. Arrows indicate positive directions of moments, forces, and angles. This system of axes is defined as an orthogonal system having the origin at the center of gravity and in which the Z-axis is in the plane of symmetry and perpendicular to the relative wind, the X-axis is in the plane of symmetry and perpendicular to the Z-axis, and the Y-axis is perpendicular to the plane of symmetry. At a constant angle of attack, these axes are fixed in the airplane.

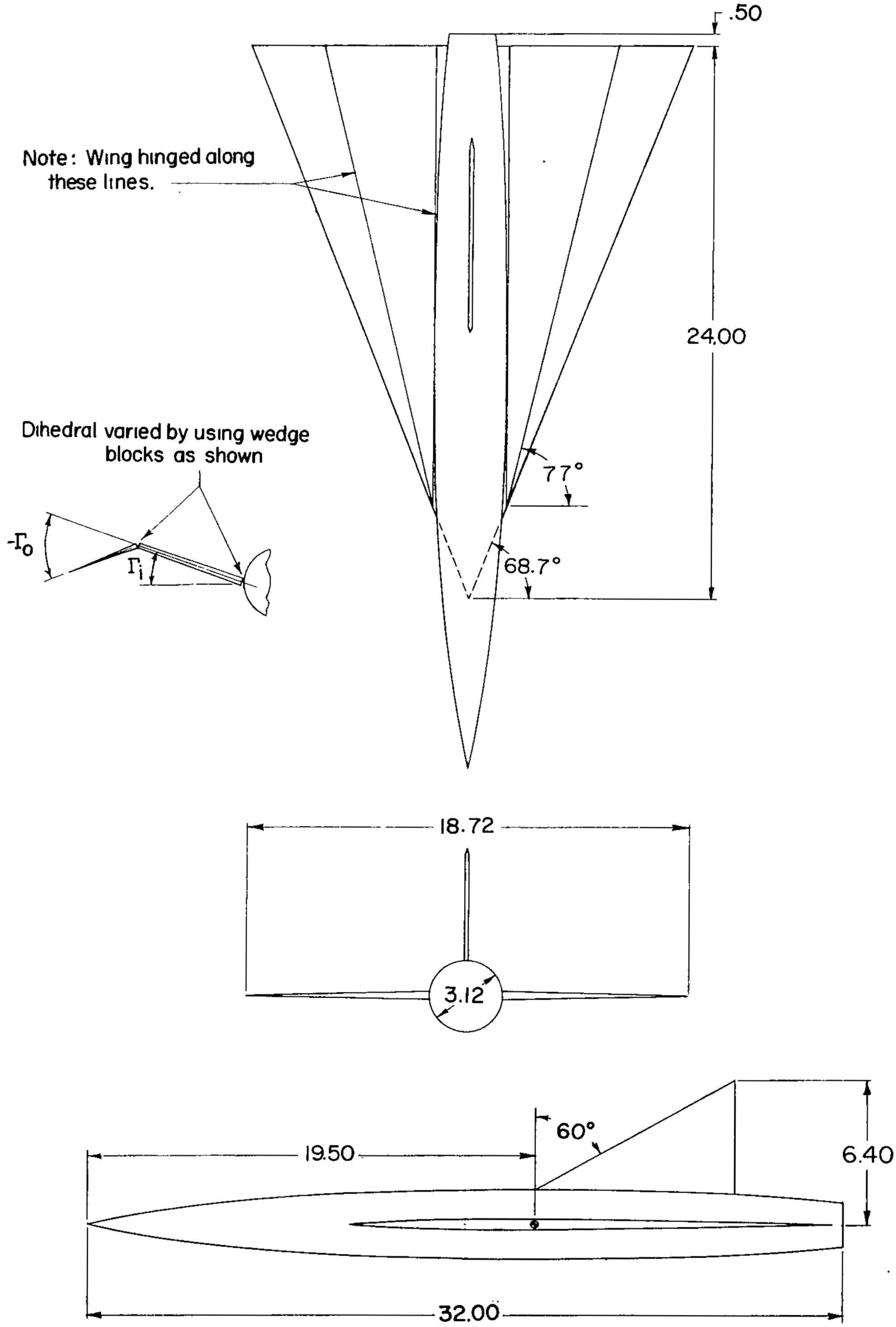

Figure 2.- Sketch of the model used in the investigation. All dimensions are in inches.

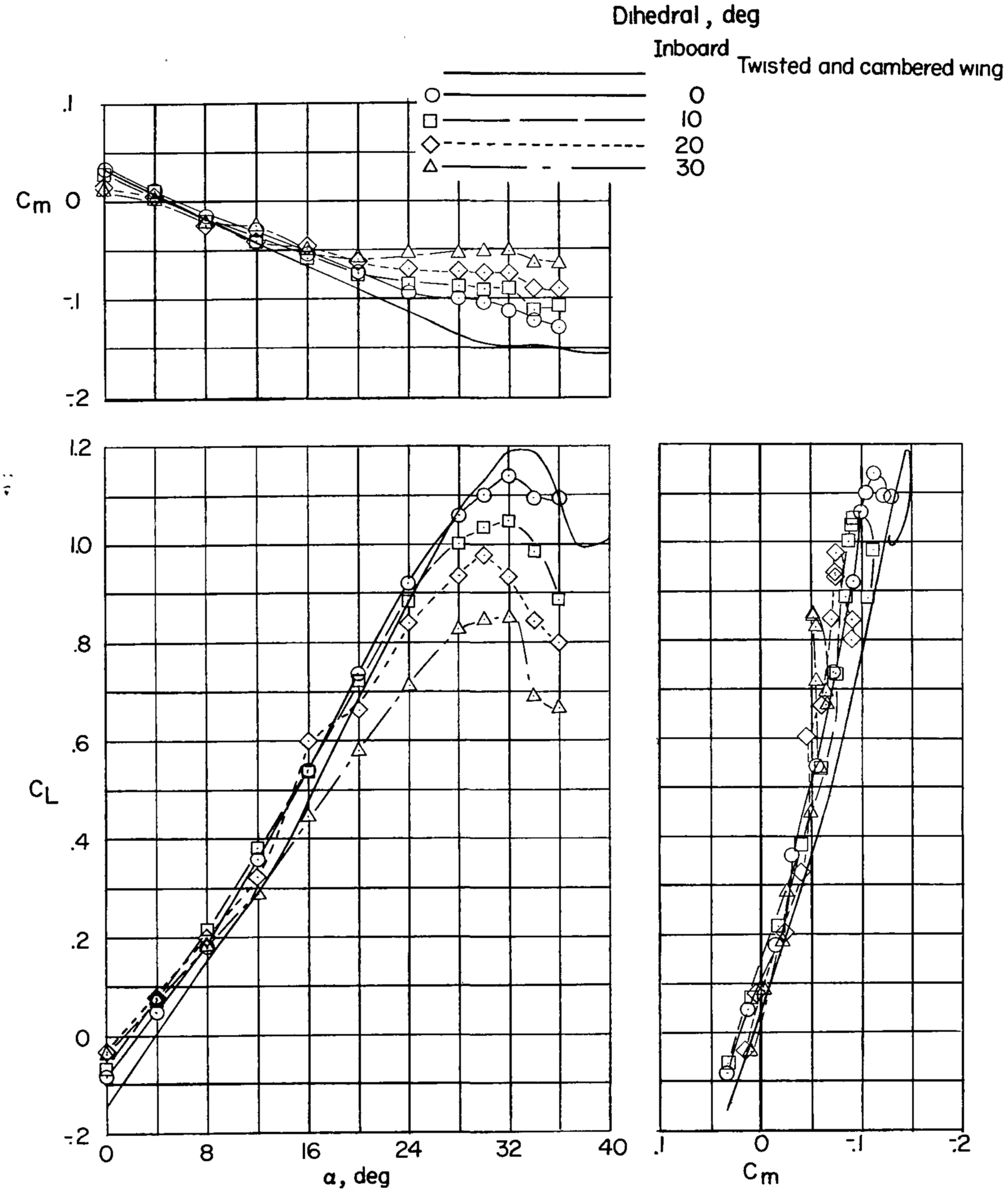

Figure 3.- Effect of inboard dihedral on longitudinal characteristics of plane-wing model. Outboard dihedral 0°; $\beta = 0^{\circ}$.

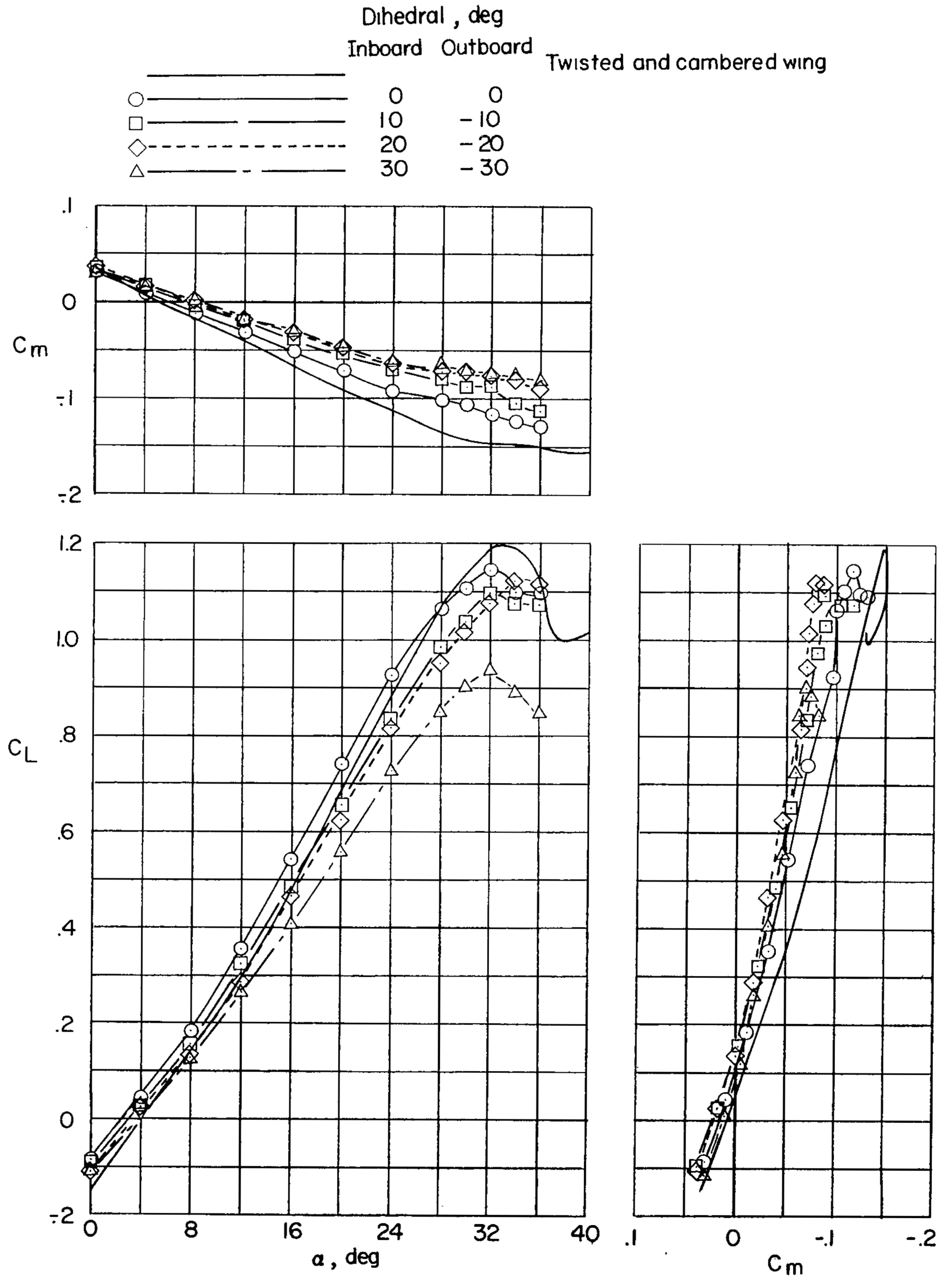

Figure 4.- Comparison of longitudinal characteristics of plane-wing model and twisted and cambered wing model. $\beta = 0^o$.

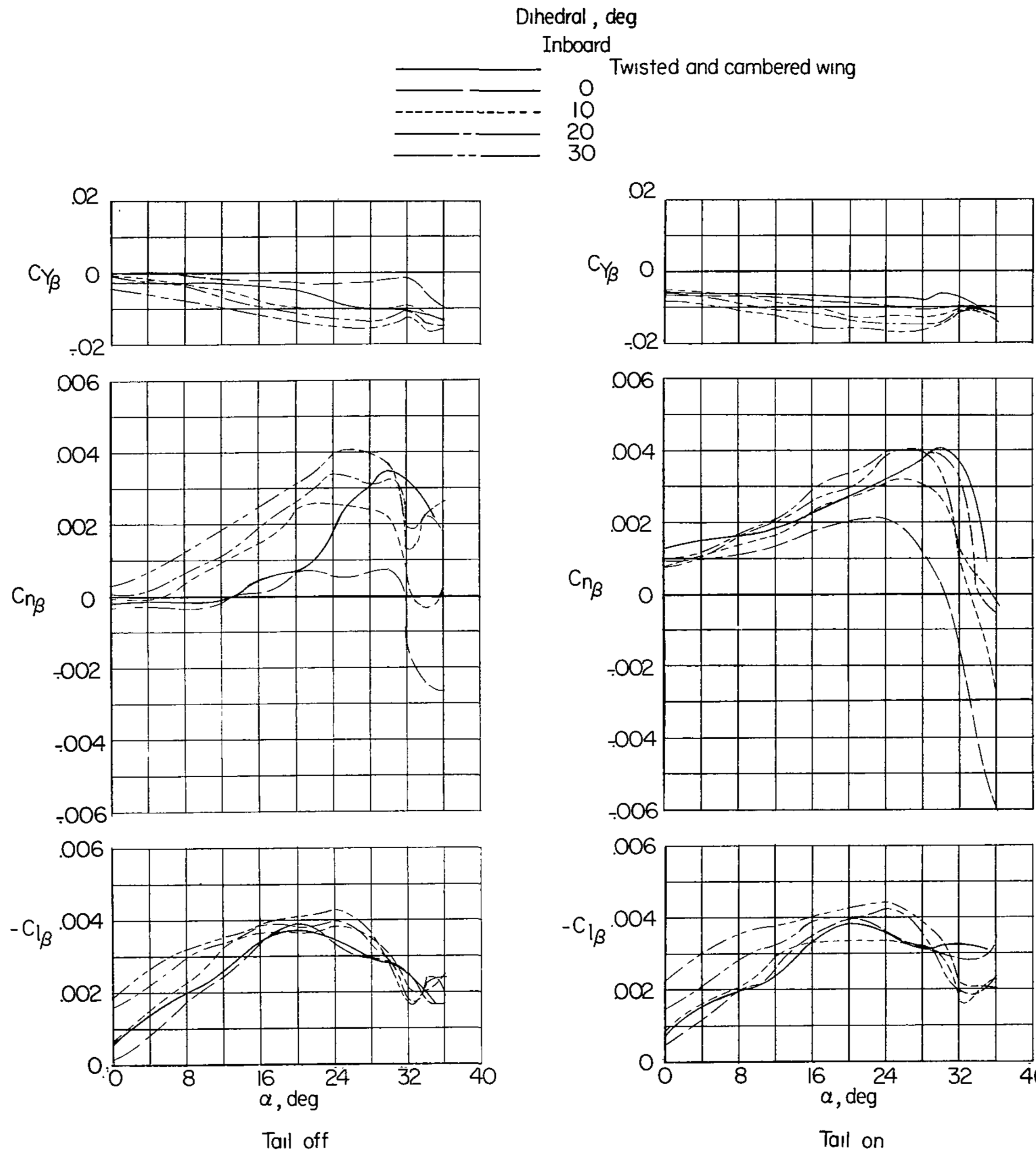

Figure 5.- Comparison of static lateral stability characteristics of plane-wing model and twisted and cambered wing model. Outboard dihedral 0°.

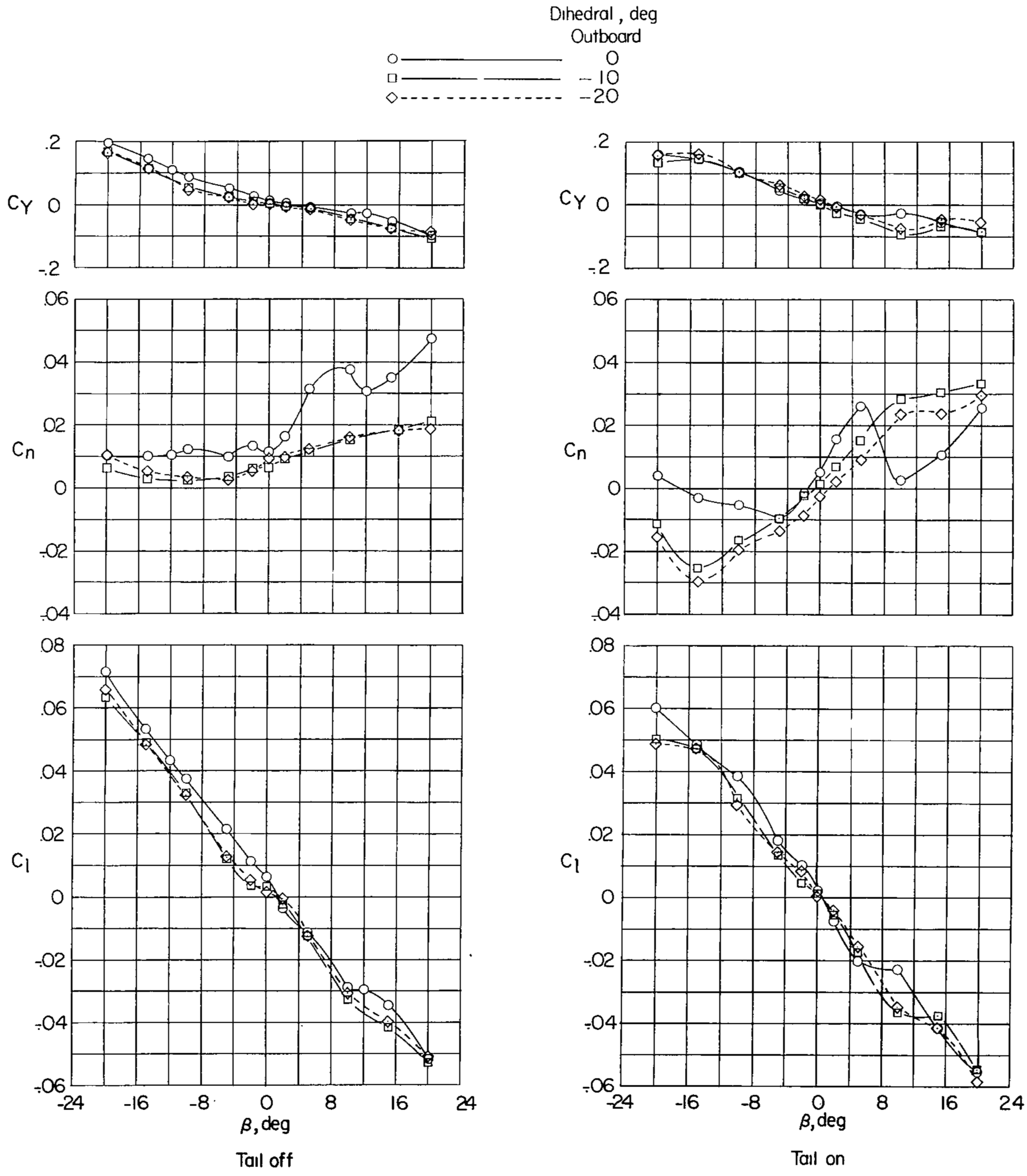

(a) Inboard dihedral 10°.

Figure 6.- Variation of the static lateral stability coefficients with angle of sideslip. $\alpha = 28^{\circ}$.

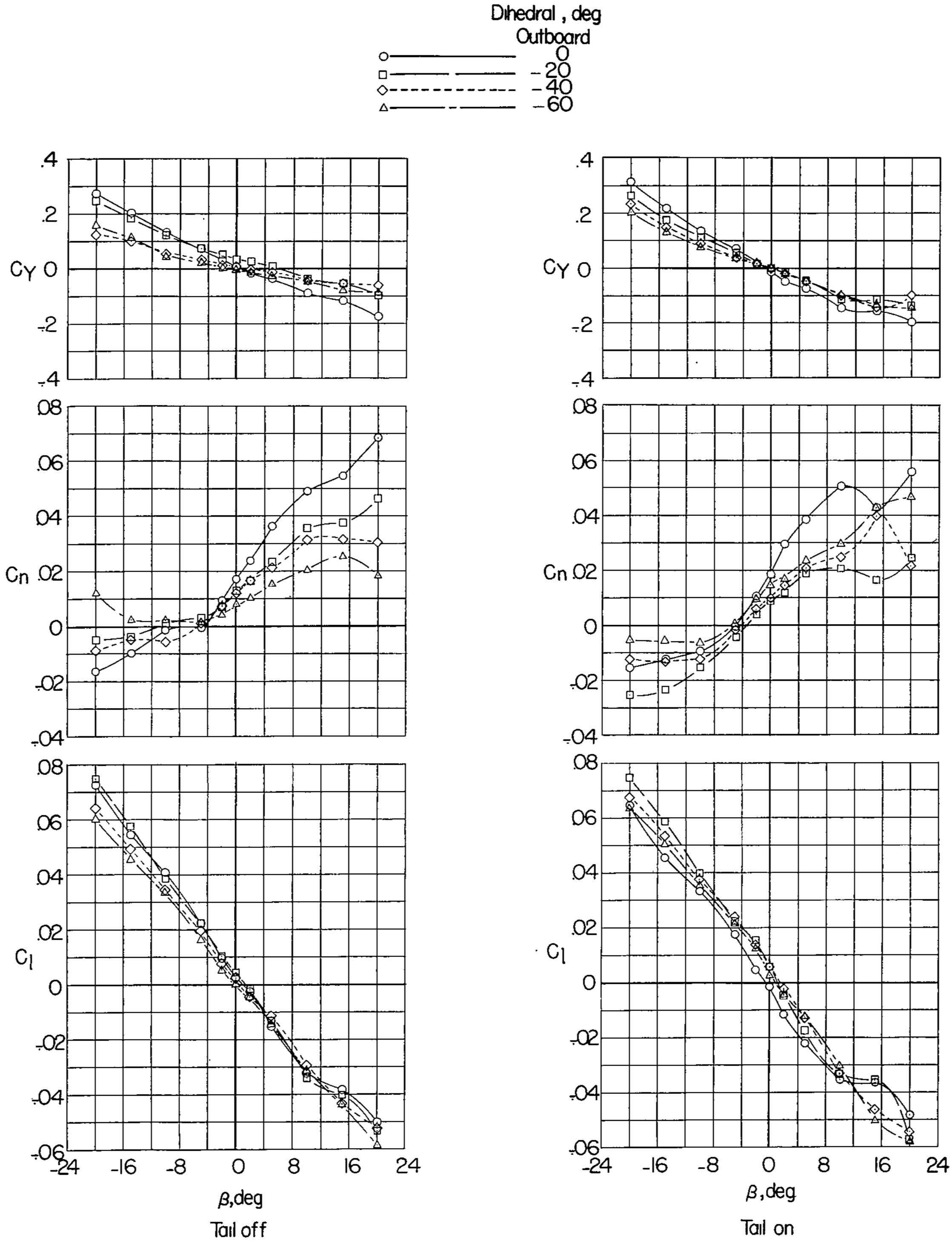

(b) Inboard dihedral 20°.

Figure 6.- Continued.

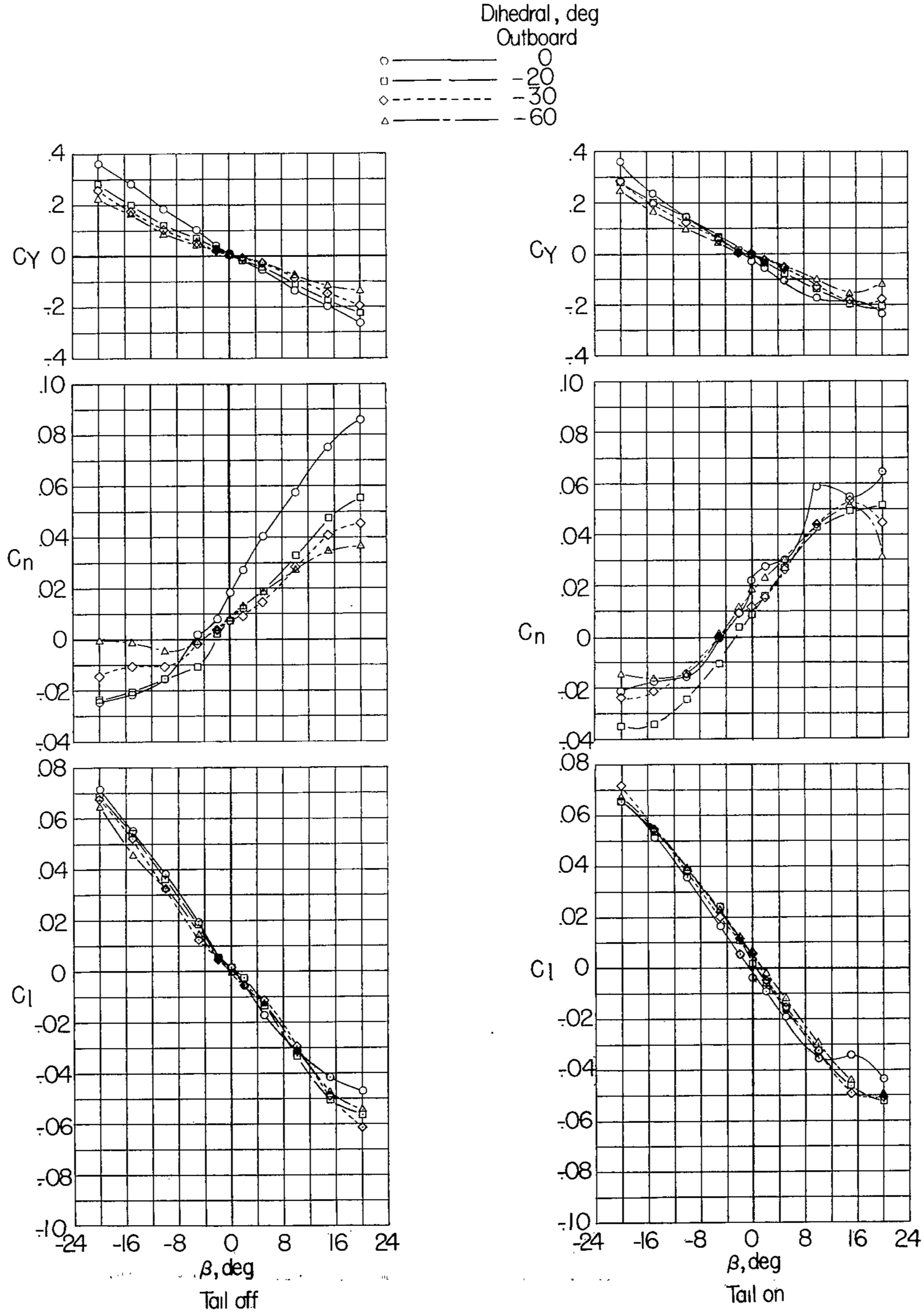

(c) Inboard dihedral 30°.

Figure 6.- Concluded.

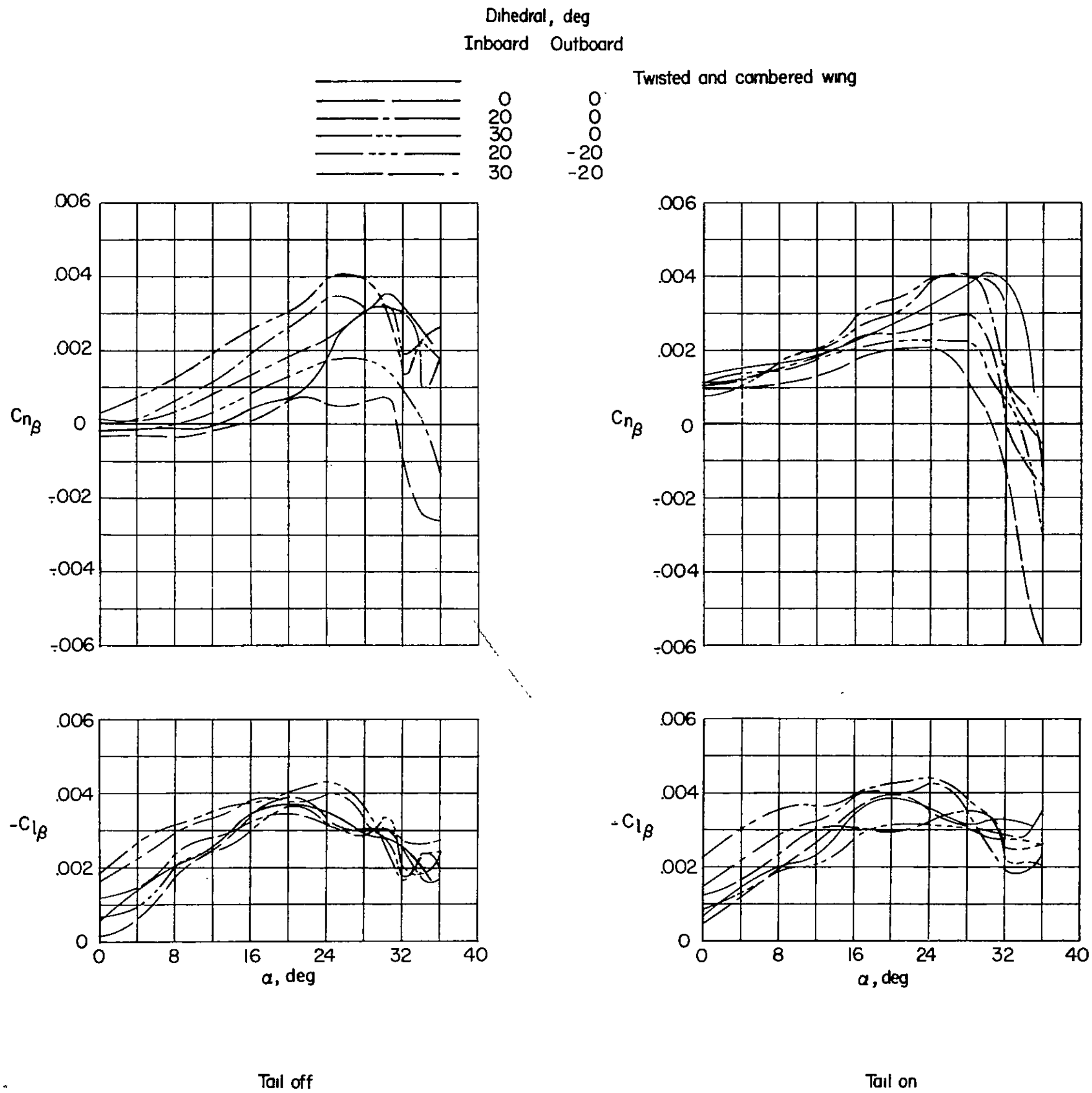

Figure 7.- Effect of various inboard and outboard dihedrals on the static lateral stability characteristics.

[redacted]

[redacted]